Electron acceleration from underdense plasma with the Vulcan Petawatt laser

S. R. Nagel, S. P. D. Mangles, P. M. Nilson, M. C. Kaluza, A. G. R. Thomas, L. Willingale, Z. Najmudin, A. E. Dangor and K. Krushelnick
The Blackett Laboratory, Imperial College London, Prince Consort Road, London, SW7 2BW, UK

R. J. Clarke
Central Laser Facility, CCLRC Rutherford Appleton Laboratory, Chilton, Didcot, Oxon., OX11 0QX, UK

N. Lopes
GoLP, Instituto Superior Tecnico, Lisbon, Portugal

K. Marsh and C. Joshi
Department of Physics and Astronomy and Electrical Engineering, UCLA, Los Angeles, California 90095, USA

Main contact email address s.nagel@imperial.ac.uk

Introduction

The advance in laser technology to ultra-high intense ($\geq 10^{18}$Wcm^{-2}) short-pulse ($\leq$1 ps) lasers has made it possible to study laser-plasma interactions at ultra-high intensities. Applications include particle accelerators [1], inertial confinement fusion schemes [2] and also biological and medical technologies. In conventional particle accelerators, the electric field used to accelerate charged particles is limited by electrical breakdown, to a maximum of the order of 50MVm^{-1} [3]. Plasmas are already ionised so are unaffected by the problems associated with material breakdown at high field strength. The use of laser excited plasma oscillations to accelerate electrons was first proposed by Tajima and Dawson [1].

In the experiment described here, the main electron acceleration mechanism is the direct laser acceleration (DLA)[4,5]. Since the electric field of the laser is both transverse and oscillating, it is usually considered as being unsuitable for electron acceleration. However, at ultra-high intensities the effect of the laser magnetic field and electric and magnetic fields within the plasma can lead to an acceleration in the longitudinal direction of the laser propagation. If we assume a free electron in a plane electromagnetic wave propagating in the z direction and polarized in the x direction. In the nonlinear relativistic regime, the magnetic field curves the electron trajectory towards the z direction (compared to the linear regime, where the electron oscillates in the perpendicular (xy) plane under the action of the electric field). As a result the electron has a longitudinal as well as transverse motion with respect to the light propagation direction.

In this report we present an interaction length scan as well as density scans and an intensity scan of the high intensity laser interactions with underdense plasma. And the electron beam divergence is measured.

Experimental Setup

The experiment described, was performed using the VULCAN Petawatt Laser. The laser had a duration of (570±30)fs and energy of up to 485J on target. The operation wavelength of VULCAN is 1055nm. For this wavelength the non-relativistic critical electron density is $n_c=10^{21}$cm^{-3}. An f/3 off-axis parabolic mirror focused the laser onto the edge of a gas jet. A focal spot measurement at low power gave a FWHM of approximately 5μm, this implies intensities up to 6×10^{20}Wcm^{-2}.

The gas jet nozzle creates a gas column with a sharp interface between the gas and the surrounding vacuum. By focusing the laser into the gas, underdense plasma is formed. The plasma density can be controlled by varying the backing pressure of the gas reservoir. Helium and hydrogen were used for the shots. The electron plasma frequency of the interaction can be found by the forward Raman scattered laser spectra. From the plasma frequency, the electron density n_e can be obtained.

$$\omega_p = \sqrt{\frac{n_e e^2}{m_e \varepsilon_0}}$$

where e is the electron charge, m_e is the electron mass. The density shows a linear dependence on the backing pressure.

The electrons were measured in the direction of laser propagation at 0°. A 2mm slit was placed in front of the entrance to the electron spectrometer, to limit the angular acceptance and hence improve the energy resolution. The accelerated electrons pass through a magnetic field. The Lorentz force deflects the electrons away from their axis of propagation. In this experiment, the 0° electron spectrometer was run with field strength of 0.2T.

Experimental Results

The shape of the electron spectra observed was not purely Maxwellian, but had an increased number of electrons in a higher energy tail.

Figure 1 shows an electron spectrum taken at an electron density of $n_e \approx 4\times10^{19}$cm^{-3}. The number of electrons per MeV per steradian (log scale) is plotted versus the energy of the electrons in MeV (linear scale). The blue fit is an exponential fit, and the lower energy part of the spectrum shows Maxwellian behaviour. From the exponential fit it is possible to determine the effective temperature as 11.5MeV. The green curve is a power law fit to the spectrum, starting at an electron energy of 75MeV. The parameters for the two different fits are displayed in the graph.

Figure 2 shows the electron beam divergence at three different positions in the stack. The data for figure 2 were

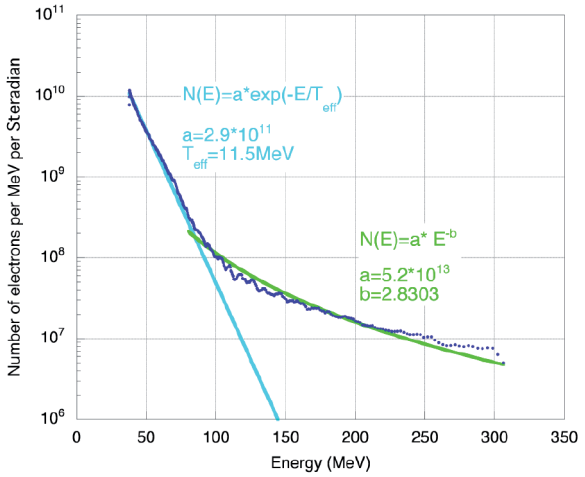

Figure 1. Electron spectrum taken at a density of $n_e \approx 4\times10^{19}cm^{-3}$ with (light blue) exponential fit and (green) power law fit to energies ≥75MeV.

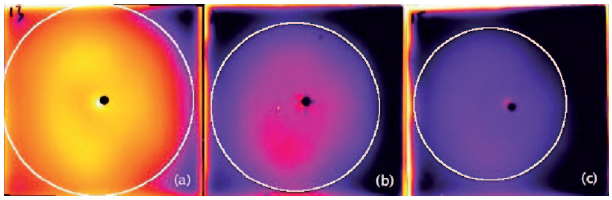

Figure 2. Image plate data of a stack for a shot taken with the same parameters as for figure 1. It shows the *electron beam divergence* at energies corresponding to, (a) ≥30MeV *0.291rad*, (b) ≥49MeV *0.197rad* and (c) ≥75MeV *0.178rad*. The beam divergence in *radians* was calculated for the FWHM.

taken at the same parameters as those for figure 1. The white circles indicate the FWHM of the Gaussians fitted to the intensity profiles. It can be seen, that the beam divergence is dependent on the energy of the electrons, and that the higher energy electrons are more collimated than the lower energy electrons. Since we are only taking a fraction of the electron beam, to measure the spectra, this may lead to the "elbow" shaped (instead of purely Maxwellian) spectra, as can be observed in figure 1.

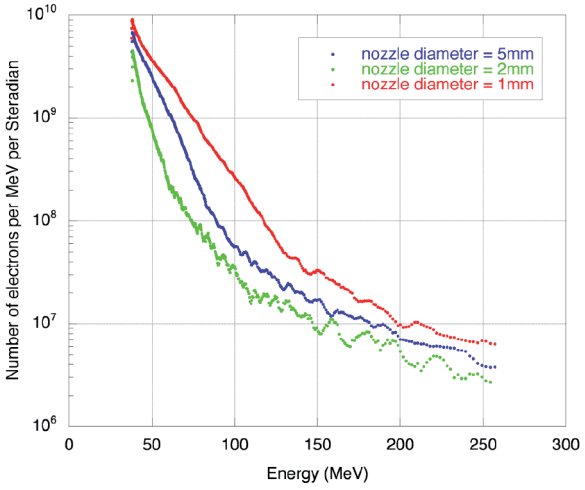

Figure 3. Comparison of the different nozzle sizes (interaction lengths), with otherwise similar parameters, at an electron density of $2\times10^{19}cm^{-3}$.

Figure 3 shows the electron spectra for three different nozzle diameters and therefore three different interaction lengths. Laser energy and electron density were kept constant as the nozzle diameter was changed. Due to the high signal level of the x-ray peak on the image plates, the maximal energy that can be resolved at the magnetic field used in these shots is around 260MeV. The spectra for the different interaction lengths look very similar and the effective temperatures are all around the order of 12MeV. This implies that the electrons are accelerated in the 1st mm. One way to achieve higher acceleration with longer interaction length is to try and access the regime of laser guiding [3]. The acceleration length may also change with the f-number [6].

In figure 4 the electron spectra for different densities are plotted. The data was taken using helium as the gas target. This density scan shows a resemblance with a scan taken in hydrogen, regarding the trends of the electron spectra. The electron spectra for the lower density shots have a higher number of electrons and go up to higher electron energies. The lower electron numbers for the higher densities (blue and green) might be due to filamenation [7]. This would reduce the efficiency of the direct laser acceleration in the direction of laser propagation.

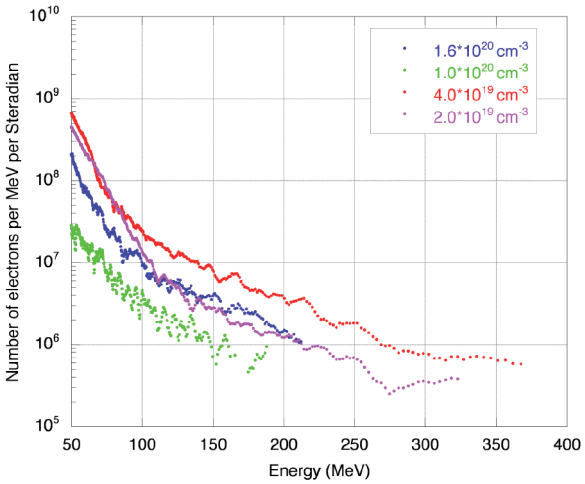

Figure 4. Density scan, with helium and a 2mm nozzle. The electron spectra were taken at the corresponding electron densities shown in the legend.

Figure 5 shows the spectra of the transmitted laser light for the helium density scan. We can see the Raman satellites changing their position with density, and a blue shift at the higher densities, that might be due to ionisation. This suggests that the Raman scattering instability growth rate was higher for the lower densities, which would explain the better acceleration.

Figure 6 shows an energy scan in hydrogen at an electron density of $2\times10^{19}cm^{-3}$. The number of electrons per steradian increases with increasing laser energy. For the highest laser energy the signal descends into the background at 420MeV. The electron energies measured in this experiment are greater than the dephasing energy ($2\gamma^2mc^2 \approx 50$ MeV). This implies that the electrons must be accelerated by a DLA mechanism. These measurements are the highest energies yet produced by direct laser acceleration.

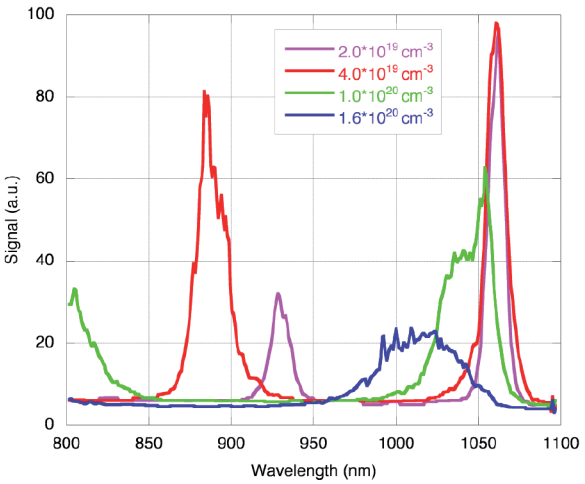

Figure 5. Optical spectrums for the He density scan.

The inset shows that the temperature of the Maxwellian component of the electron beam increases with laser energy. T_{eff} doubles, as a_0, the normalised vector potential, doubles. This intensity dependence also implies DLA. However, the fit from which we obtained the effective temperatures only fits the lower energy parts of the spectra. This two-temperature shape of the spectrum indicates a two-stage acceleration. DLA depends on a preacceleration, which accelerates electrons to velocities, where they can reach the resonant behaviour. Previously this preaccelertaion was attributed to SMLWA[4], but the strong intensity dependence observed here suggests that DLA is also important for the lower energy electrons (above 50-80MeV). This may be in the form of a stochastic acceleration. In order to understand these acceleration processes fully particle-in-cell simulations are in progress.

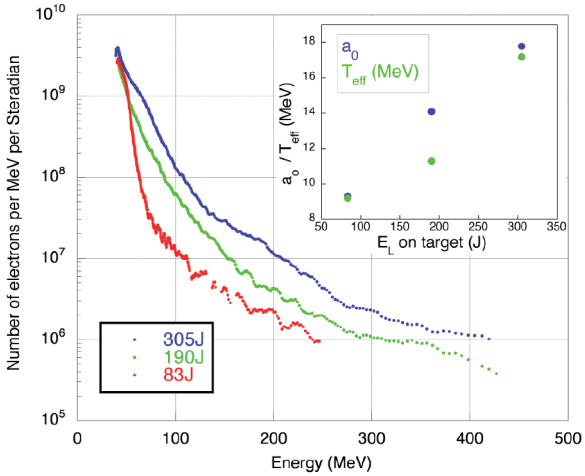

Figure 6. Energy scan, with hydrogen and a 2mm nozzle. The electron spectra were taken at the corresponding energies on target shown in the legend. (The inset shows the effective temperature and normalised vector potential vs. the laser energy on target.)

Conclusions

The shape of the electron spectra is partly due to the energy dependent electron beam divergence. Further measurements will be necessary to determine if this energy dependent beam divergence changes with the electron density and/or laser intensity, and why it has changed from the Maxwellian distribution in other experiments to the "elbow" shaped spectra in this one. Possible reasons for the latter could be less filamentation or better alignment of the spectrometer.

In order to get better insight into the processes leading to the trends observed in the density and intensity scans, further analysis and comparisons with other experiments, as well as computer simulations are under way.

Acknowledgements

The authors acknowledge the assistance of the Central Laser Facility staff at the Rutherford Appleton Laboratory in carrying out this work. This work was supported by the UK Engineering and Physical Sciences Research Council (EPSRC).

References

1. T. Tajima and J. M. Dawson, *Phys. Rev. Lett*. **43**, 267 (1979)
2. M. Tabak *et al*., *Phys. Plasmas* **1**, 1626 (1994)
3. E. Esarey *et al*., *IEEE Trans. Plas. Sci.* **24**, 252 (1996)
4. S. P. D. Mangles *et al*., *Phys. Rev. Lett.* **94**, 245001 (2005)
5. A. Pukhov and J. Meyer-ter Vehn, *Physics of Plasmas* **5**, 1880 (1998)
6. A. G. R. Thomas, *Phys. Rev. Lett.* submitted (2006)
7. S. P. D. Mangles, *RAL CLF Annual Report 2005/2006*